sustainability

MDPI

Article

Waste Brick as Partial Replacement of Gypsum in Mortars: Mechanical Performance and Environmental Benefits for Sustainable Construction

Said Beldjilali [1], Antonella Sarcinella [2,*], Mohamed Amine Ouared [3], Abdelkader Bougara [3], Khalil Naciri [4] and Rodica-Mariana Ion [5,6]

1 Department of Architecture, University Abdelhamid Ibn Badis of Mostaganem, Mostaganem 27000, Algeria; said.beldjilali@univ-mosta.dz
2 Innovation Engineering Department, University of Salento, Prov. le Lecce-Monteroni, 73100 Lecce, Italy
3 Laboratory of Structures, Geotechnics and Risks, University of Chlef, Chlef 02000, Algeria; m.ouared@univ-chlef.dz (M.A.O.); a.bougara@univ-chlef.dz (A.B.)
4 National Higher School of Arts and Crafts (ENSAM), Moulay Ismail University, Marjane 2, Al Mansour, Meknes P.O. Box 15290, Morocco; k.naciri@est.umi.ac.ma
5 National Institute of R&D for Chemistry and Petrochemistry (ICECHIM), 202 Splaiul Independentei, 060021 Bucharest, Romania; rodica_ion2000@yahoo.co.uk
6 Doctoral School of Materials Engineering Department, University Valahia of Targoviste, 13, Aleea Sinaia, 130004 Targoviste, Romania
* Correspondence: antonella.sarcinella@unisalento.it; Tel.: +39-3291892346

Abstract

Replacing virgin raw materials with recycled waste in construction products is a key strategy for advancing sustainable development. This study explores the partial substitution of commercial gypsum with powdered waste brick (WB) in gypsum mortars, assessing its impact on mechanical performance, water absorption, and environmental footprint. Mortars were prepared with 0%, 5%, 10%, 20%, and 30% WB by weight. Results indicate that a 20% replacement level enhances flexural strength by 56% and compressive strength by 33% at 28 days, compared to the reference mix. SEM and XRD analyses revealed no formation of new crystalline phases, suggesting that the performance improvement is primarily due to physical interactions and microstructural effects. However, at 30% WB, a significant reduction in adhesion strength was observed, falling below the typical threshold for gypsum-based coatings, which may constrain practical application at higher replacement levels. Environmental assessment showed that both CO_2 emissions and energy consumption decreased by up to 20% with a 30% substitution. A 20% WB content is therefore proposed as the optimal compromise between mechanical performance and environmental benefit. This approach supports circular economy principles by promoting the reuse of ceramic construction waste in the development of new sustainable materials.

Keywords: gypsum mortar; waste brick; sustainable construction material; mechanical and environmental performance; partial binder replacement

Academic Editor: José Ignacio Alvarez

Received: 10 July 2025
Revised: 9 August 2025
Accepted: 12 August 2025
Published: 18 August 2025

Citation: Beldjilali, S.; Sarcinella, A.; Ouared, M.A.; Bougara, A.; Naciri, K.; Ion, R.-M. Waste Brick as Partial Replacement of Gypsum in Mortars: Mechanical Performance and Environmental Benefits for Sustainable Construction. *Sustainability* **2025**, *17*, 7452. https://doi.org/10.3390/su17167452

1. Introduction

The construction industry generates vast amounts of construction and demolition waste (CDW) each year [1]. China alone produces an estimated 1.8 billion tons annually (approximately 23% of the global total), followed by Europe (8%), and the United States (7%), with no signs of a declining trend [2–4]. Among the various components of CDW,

ceramic waste (i.e., bricks, tiles, terracotta fragments) accounts for a substantial share, reaching up to 50% in some cases. Despite this, large-scale and effective recycling strategies for ceramic waste remain limited [5]. This growing accumulation poses both an environmental challenge and an opportunity. Reusing waste bricks (WBs), for example, can reduce landfill burden, reduce reliance on non-renewable raw materials, and contribute to the mitigation of greenhouse gas emissions [6,7]. As a result, interest is growing in circular-economy approaches aimed at valorizing these materials rather than discarding them.

Currently, WB has primarily been used as a recycled aggregate in concrete or mortar. For instance, Zhou et al. [8] processed waste clay bricks into both powder and coarse particles to manufacture specialized plastering mortars with improved long-term shrinkage and strength. The powder promoted pozzolanic reactions, while the coarser fraction contributed to internal curing effects and increased durability, particularly when combined with styrene-butadiene latex for consistency enhancement. The study emphasized the dual role of WB as both aggregate and reactive filler in mortar systems. Similarly, Raini et al. [9] incorporated brick powder as a partial replacement for lime and combined it with recycled concrete aggregates (RCAs) to produce eco-friendly lime mortars. The incorporation of 30% brick powder improved compactness and water resistance due to its pozzolanic activity, while the optimized use of RCA reduced density and supported the development of restoration mortars for historic buildings. These findings collectively demonstrate the technical feasibility and sustainability benefits of reusing ceramic waste in mortar formulations, particularly as aggregates or partial binder substitutes. Beyond their use as aggregate, crushed bricks are often employed as substitutes for sand or gravel in non-structural applications such as sub-base layers or low-performance concrete, thereby further extending their reuse potential [10,11].

A more advanced and promising strategy has recently emerged: grinding brick waste into a fine powder to partially replace cementitious binders. Several studies have demonstrated that finely ground WB can exhibit pozzolanic activity, especially when the original firing process has produced amorphous silica and alumina. When incorporated into mortar or concrete at replacement levels up to 20%, WB powder can improve compressive and flexural strength by promoting secondary hydration reactions [5]. Similarly, Guo et al. [12,13] showed that using thermally activated red mud powder, rich in aluminosilicates, in alkali-activated systems can achieve compressive strengths up to 33.5 MPa, with improved microstructure and reduced shrinkage, highlighting the broader potential of industrial powders in sustainable binder formulations. These examples point to a growing trend of utilizing industrial and ceramic by-products not only to reduce waste, but to enhance performance characteristics in sustainable construction materials.

This approach not only supports waste valorization, but also contributes to reducing the carbon footprint of construction materials by lowering the demand for high-CO_2 binders such as Portland cement.

In one recent study, Chen et al. investigated the use of recycled clay brick powder (RCBP) as supplementary cementitious material in hybrid mortars containing recycled glass and brick aggregates [14]. The authors demonstrated that replacing 30% of cement with RCBP resulted in a 28-day activity index close to 97%, confirming the material's pozzolanic reactivity. Although higher substitution levels slightly reduced compressive strength and workability, the study confirmed the feasibility of integrating recycled materials in the formulation of a durable and sustainable mortar. Another study performed by Kilumile et al. [15] investigated the performance of historical lime-based mortars incorporating recycled burnt clay brick sand and recycled concrete sand as fine aggregates. When compared with a control mortar made with natural river sand, the mortar containing the recycled aggregates showed significantly enhanced mechanical properties. After 28 days, its

flexural strength was 300% higher than that of the control mix, while compressive strength followed a similar trend. These findings emphasize the recycled brick aggregates can not only reduce environmental impact, but also enhance mechanical performance, particularly in the context of repair mortars for historical masonry.

More recently, a novel research direction has emerged: using waste brick powder not merely as an aggregate, but as a partial binder replacement in cementitious systems [16,17]. This shift in approach underlines the evolving role of ceramic waste in sustainable material formulations. Building upon these promising results, this research explores whether similar benefits can be achieved in gypsum-based mortar. Gypsum is already considered a more environmentally friendly alternative to cement due to its lower calcination temperature (around 150 °C), which results in reduced energy consumption and CO_2 emissions (approximately 820 MJ/t and 100–140 kg CO_2/t, respectively) [18,19]. Gypsum mortars have recently regained attention in sustainable construction, not only for restoration purposes but also as a base for eco-friendly plasters incorporating recycled materials [20,21]. However, further environmental benefits may be achieved by replacing a portion of gypsum with ceramic waste, thereby combining two sustainability goals: waste reduction and decreased raw material demand.

While many studies have examined the incorporation of CDW as inert filler or reinforcement in gypsum composites, relatively few have explored the direct replacement of gypsum itself with such materials. For example, Beldjilali et al. [22] demonstrated that WB powder can partially replace gypsum without triggering any significant chemical reactions, while still improving key mechanical properties (flexural, compressive, and adhesion strength), most likely through particle packing and improved microstructure density. Similarly, Naciri et al. [23] showed that incorporating WB into gypsum-lime mortars can enhance their mechanical behavior both in dry and saturated conditions.

In terms of sustainability, replacing gypsum with WB offer multiple benefits: it reduces energy consumption during binder production, lowers CO_2 emissions in the final product, and aligns with circular construction principles by reintegrating ceramic waste into new material cycles. This approach also helps limit raw gypsum extraction and decreases landfill accumulation.

In this context, the present research investigates the use of WB as a partial replacement for gypsum in mortar formulations. Five mixtures were prepared with 0%, 5%, 10%, 20%, and 30% WB by weight. A comprehensive experimental program was conducted to assess setting time, water absorption, compressive and flexural strength, adhesion to limestone substrate, and microstructural analysis (SEM, EDS, XRD). Additionally, the environmental performance of each mixture was assessed based on CO_2 emissions and energy demand.

This work proposes an innovative valorization route for ceramic CDW (i.e., waste bricks) and aims to identify the optimal gypsum replacement level that balances mechanical performance and environmental benefit, thereby contributing to the development of eco-efficient mortars suitable for both construction and restoration applications.

2. Materials and Methods

2.1. Materials

The materials used in this study include commercial gypsum (G), construction sand (CS), recycled waste brick powder (WB), and a superplasticizer (SP). The gypsum was a high-fineness commercial product supplied by RIGIPS (Turda, Romania), in compliance with EN 13279-1 [24]. The sand, supplied by ADE-PLAST (Oradea, Romania), was a quartz-based aggregate, with a density of 2600 kg/m^3 and water absorption of 5.4%.

The waste bricks were sourced from Cemacon (Zalău, Romania), a local supplier of construction demolition waste. After initial coarse crushing, the material was finely ground

and sieved to obtain a powder with particles smaller than 1 mm, of which approximately 70% were below 0.25 mm. This particle size distribution was selected to promote filler effects and improve matrix densification. The particle size distribution of sand and waste brick powder is shown in Figure 1.

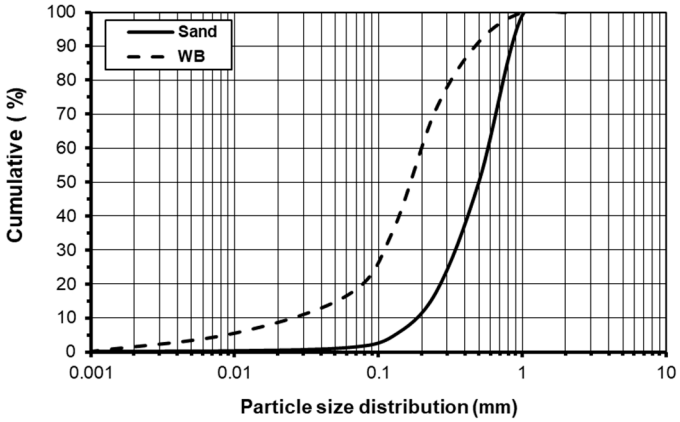

Figure 1. Particle size distribution of sands and WB.

In particle size distribution (PSD) analysis, D10, D50, and D90 are key parameters that represent specific particle size percentiles. D10 is the particle size below which 10% of the particles in a sample fall, D50 is the median particle size (50% of particles are smaller, 50% are larger), and D90 is the particle size below which 90% of the particles fall. For sand, we obtain the following data: D10 ≈ 0.18 mm; D50 ≈ 0.45 mm; D90 ≈ 0.85 mm, while for WB, the data are D10 ≈ 0.03 mm; D50 ≈ 0.20 mm; D90 ≈ 0.50 mm.

A polycarboxylate-based superplasticizer (Sika Plastiment BV540 Super, density 1050 kg/m^3, Sika AG, Baar, Switzerland) was used to improve workability and ensure consistent flow across all mixtures.

The chemical composition and mineralogical characteristics of the raw materials were analyzed using X-ray fluorescence (XRF) and X-ray diffraction (XRD), respectively.

XRD analysis was performed using a Rigaku Ultima IV X-ray diffractometer (Rigaku Corporation, Tokyo, Japan), equipped with Cu-Kα radiation (λ = 0.15406 nm), at 40 kV and 30 mA. Data were collected over a 2θ range of 5–100° with a step size of 0.0200° and a scanning speed of 1°/min. The instrument, fitted with a NaI detector (count rate limit > 700,000 cps), supports both symmetric and asymmetric geometries, including high-resolution Bragg–Brentano and parallel beam configurations, with a minimum step width of 0.001 mm. Data acquisition and processing were performed using PDXL 2.2 software in conjunction with the ICDD PDF-4+ 2016 database.

Phase identification was carried out based on standard patterns from the ICDD database, specifically using category S (Star Patterns—extremely high-quality data) and category I (Indexed Patterns—indexed high-quality data). The detection limit of the XRD method is approximately 1%. The XRD patterns of sand, gypsum, and waste brick are shown in Figure 2.

The main crystalline phases identified include quartz, microcline, petalite, cristobalite, stishovite, and iron in the sand; bassanite as the dominant phase in gypsum, with minor anhydrite and berlinite; and quartz and albite in the WB, along with traces of sodalite and titanium oxide (Ti_8O_{15}).

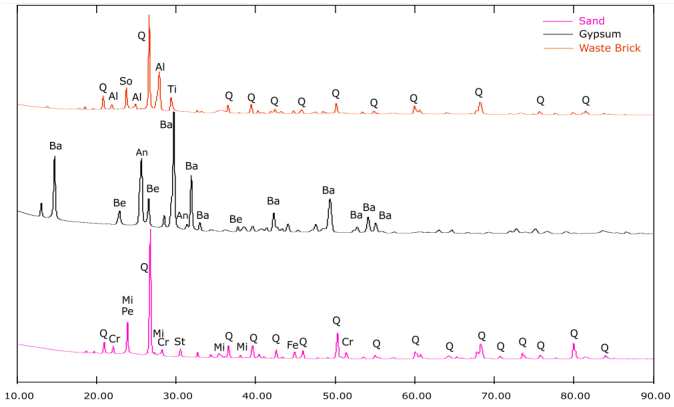

Figure 2. XRD patterns of sand, gypsum, and WB (Al: albite (COD: 2107372), An: anhydrite (COD: 5000040), Ba: basanite (COD: 1010918), Be: berlinite (COD: 1531951), Cr: cristobalite (COD: 1010921), Fe: iron (COD: 9013463), Mi: microcline (COD: 9000943), Pe: petalite (COD: 9008304), Q: quartz (COD: 1011097), So: sodalite (COD: 1011139), St: stishovite (COD: 1544731), Ti: Ti_8O_{15} (COD: 1520782)).

Elemental composition was determined by wavelength-dispersive XRF, using a Rigaku ZSX Primus II spectrometer (Rigaku Corporation, Tokyo, Japan), equipped with an Rh-anode X-ray tube (4.0 kW) and a 30 µm beryllium window, operating under vacuum conditions. Samples were prepared as pressed pellets. The resulting chemical composition, as well as the density and water absorption of each raw material, are presented in Table 1.

Table 1. Chemical composition and characteristics of the materials used.

Component	Construction Sand (%)	Gypsum (%)	WB (%)
Na_2O	0.00	0.24	1.44
MgO	1.36	0.05	1.70
Al_2O_3	18.86	1.02	13.68
SiO_2	64.40	2.38	44.08
P_2O_5	0.00	0.06	0.15
SO_3	0.94	57.91	9.13
Cl	0.22	0.00	0.05
K_2O	4.99	0.18	1.92
CaO	1.62	37.57	20.13
TiO_2	0.00	0.00	0.64
MnO	0.00	0.00	0.16
F_2O_3	6.31	0.30	6.68
ZnO	0.91	0.00	0.13
Rb_2O	0.15	0.00	0.00
SrO	0.24	0.28	0.07
ZrO_2	0.00	0.00	0.06
Density (kg/m^3)	2600	2960	2700
Water absorption (%)	5.40	2.50	28.90

As expected, gypsum exhibited high CaO and SO_3 contents, whereas the WB powder showed a significantly higher proportion of SiO_2 and lower SO_3 content. Notably, WB also demonstrated a much higher water absorption capacity (28.9%) compared to gypsum (2.5%), which is expected to influence both the rheological behavior and mechanical performance of the resulting mortar mixes.

2.2. Mix Design

Five mortar formulations were developed by partially replacing gypsum with waste brick powder (WB) at weight-based substitution levels of 0%, 5%, 10%, 20%, and 30%, identified as M1 through M5, respectively. These levels were selected to represent a range from low (5% and 10%) to high (20% and 30%) incorporation rates, while limiting the

number of tested mixtures. The 30% replacement level is commonly reported in the literature as the upper limit for maintaining workability and cohesion, despite notable reductions in mechanical strength [16]. The 20% level is widely considered a threshold for preserving acceptable performance. Each formulation contained a fixed amount of construction sand and superplasticizer. Water content was adjusted across mixtures to maintain a similar level of workability, with target flow values ranging from 160 to 180 mm, in accordance with EN 1015-3 [25]. All mixtures were prepared under laboratory conditions.

The component quantities, expressed in kg/m^3, are detailed in Table 2. It is important to note that the values reported for gypsum content (ranging from 800 to 560 kg/m^3) are not experimental design variables, but rather result from the progressive replacement of gypsum with WB powder (from 0% to 30% by weight). As the gypsum content decreases, the amount of mixing water is also adjusted; however, not proportionally, resulting in an increase in the water-to-gypsum (W/G) ratio from 0.40 to 0.55. The contents of sand and superplasticizer were kept constant across all mixtures to ensure comparability in terms of workability and volume consistency.

Table 2. Component of the mortar mixtures expressed in kg/m^3.

Sample	Gypsum	WB	Sand	SP	Water	W/G
M1	800	0.0	967.20	40	320	0.40
M2	760	36.49	967.20	40	342	0.45
M3	720	72.97	967.20	40	360	0.50
M4	640	145.95	967.20	40	352	0.55
M5	560	218.92	967.20	40	308	0.55

2.3. Sample Preparation

All dry components (G, WB, and CS) were first manually premixed and then homogenized in a mechanical mixer. Water and superplasticizer were added gradually, and the final mortar was mixed until uniform consistency was achieved, in accordance with the standard EN 998-1 [26]. In order to test the mortar samples, nine prismatic specimens ($40 \times 40 \times 160$ mm^3) were cast for each mortar formulation according to the European specification 1015-11 [27].

At first, the molds were filled with the fresh mortar in two roughly equal layers. They were then sealed with a sheet of polyethylene. After 48 h, the samples were demolded and placed in polyethylene bags for an additional five days, maintained at approximately 20 °C and 95% relative humidity. Following this initial curing stage, the specimens were stored under standard laboratory conditions (around 20 °C and 65% relative humidity) for a further 21 days. Although these curing conditions differ from those specified in EN 13279-1 [24] (which recommends 40 °C), they were chosen to better simulate indoor environmental exposure and to ensure consistency across all tests, including mechanical strength, water absorption, and adhesion.

However, mechanical testing was performed at three different curing intervals: 7, 14, and 28 days. For the adhesion strength tests, three cylindrical samples (50 mm in diameter) were prepared for each mortar formulation and exposure condition, in accordance with EN 1015-12 [28]. Fresh mortar was applied in 15 mm thick layers onto limestone substrate, chosen due to their use in Romanian historical buildings. The composite specimens were initially covered with polyethylene film and cured for seven days at about 20 °C and 95% relative humidity. After this curing period, the film was removed, and the samples were conditioned in laboratory air (20 °C, 65% RH). A circular cut of 50 mm diameter was then made on each specimen, and a metal disc of the same size was glued to the surface of the mortar to prepare for the pull-off adhesion test.

2.4. Testing Methods

A comprehensive experimental program was carried out to evaluate the physical, mechanical, and microstructural properties of the gypsum-based mortars. Physical performance was assessed through setting time measurement and water absorption by immersion, while mechanical behavior was evaluated via flexural, compressive, and adhesion strength tests. Microstructural characterization included optical microscopy, scanning electron microscopy (SEM), energy-dispersive X-ray spectroscopy (EDS), and X-ray diffraction (XRD).

Setting time was determined using a Vicat apparatus (Vicat SA, Saint-Égrève, France), in accordance with the corresponding standard [29]. Water absorption by immersion was measured by recording the dry mass of specimens and their mass after 24 h of immersion in distilled water. For this test, half-prisms obtained from the 28-day flexural tests were used. Prior to testing, samples were oven-dried at 50 ± 5 °C until constant mass, in compliance with standard [30].

Mechanical strength tests included three-point bending tests on prismatic specimens and compressive strength tests on the fractured halves of the same specimens, performed at 7, 14, and 28 days according to standard [27]. Testing was performed using an MTS 100 (MTS Systems Corporation, Eden Prairie, MN, USA) loading device with a loading rate of 50 N/s for flexural strength and 2400 N/s for compressive strength. Adhesion strength was assessed by applying two 15 mm thick layers of each mortar formulation onto limestone substrates, chosen due to their common use in Romanian historical buildings [31,32]. After 28 days of curing, six circular holes with a diameter of 50 mm were cut from each mortar layer and bonded to metal discs. A perpendicular tensile load was applied until failure, following the procedure outlined in standard [28]. The equipment used for the mechanical characterization of the samples is shown in Figure 3.

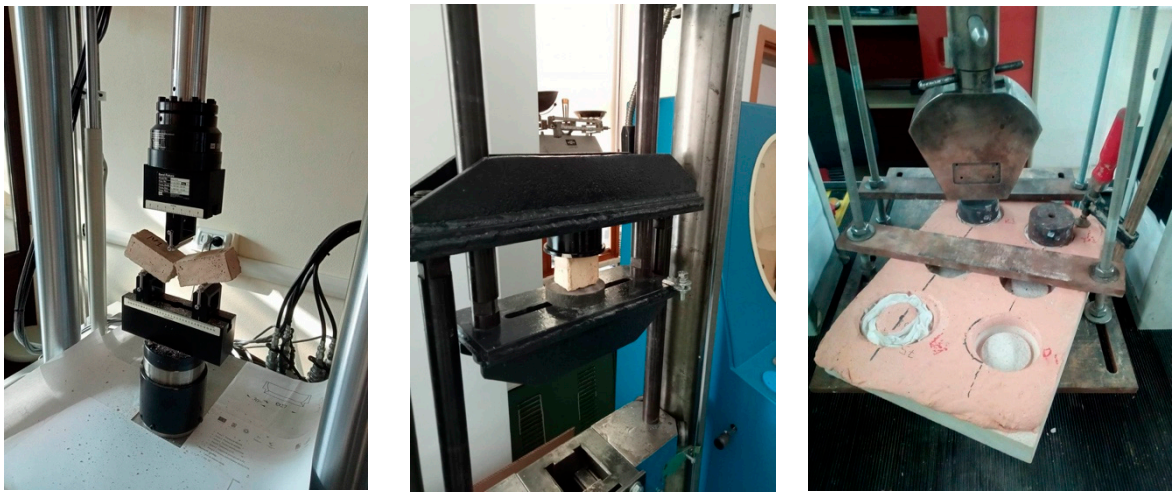

(**a**) Flexure test (**b**) Compression test (**c**) Adhesion test

Figure 3. Mechanical tests performed on gypsum-based mortar specimens with and without WB.

Optical microscopy was performed with a Novex trinocular microscope (EUROMEX Microscopen B.V., Arnhem, The Netherlands) to examine the surface homogeneity of the mortars. SEM analysis, carried out with an SU-70 microscope (Hitachi, Tokyo, Japan), allowed for detailed observation of the microstructural morphology. The SEM operated at accelerating voltages ranging from 0.1 kV to 30 kV, with magnifications between 30× and 800,000×, and a resolution of 1 nm at 15 kV. EDS was employed for elemental microanalysis, while XRD was used, as previously described, to identify the mineralogical composition of the mortar mixtures.

2.5. Environmental Assessment

The environmental performance of the different mortar formulations was evaluated by estimating the associated CO_2 emissions (i.e., Global Warming Potential, GWP) and energy demand, adopting a cradle-to-gate approach. Emission and energy factors were derived from the literature, and the functional unit was set as 1 m^3 of hardened mortar, to allow a fair comparison among the mixtures.

The GWP for each mortar mix was calculated using the following Equation (1):

$$GWP_{mortar} = \sum_i \left(\frac{m_i}{1000} \cdot EF_i \right) \quad (1)$$

where m_i is the mass (in kg) of component i per cubic meter of mortar, and EF_i is the emission factor of component i (expressed in kg CO_2-eq per ton of material). The same formula was applied to estimate the total energy demand, substituting emission factors with energy consumption factors (in MJ/t).

3. Results and Discussion

3.1. Setting Time

The evolution of the setting time of the gypsum mortars as a function of WB content is presented in Figure 4. The initial and final setting times were measured using the Vicat method and are defined, respectively, as the time from the initial contact between the dry components and water to a penetration depth of the 22 mm, and the time at which the needle no longer sinks into the material.

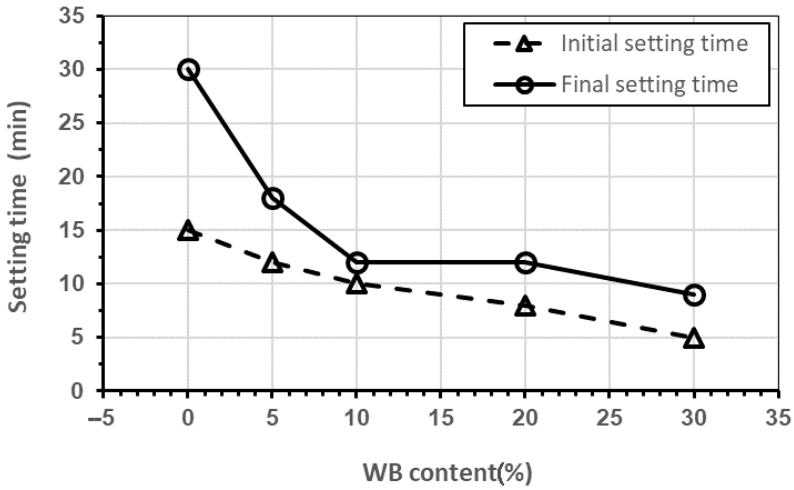

Figure 4. Mortar setting time versus WB content.

The reference mortar M1 (i.e., 0% WB) exhibited the longest setting times, with an initial setting of approximately 15 min and a final setting of around 30 min. As the percentage of WB increased, both initial and final setting times progressively decreased. Mortars M4 and M5, containing 20% and 30% WB, respectively, showed initial setting times of less than 10 min and final setting times close to 15 min for M4 and less than 10 min for M5. This trend reflects an almost linear reduction in setting time with increasing WB content. This behavior can be attributed to the high water absorption capacity of the WB particles, as shown in Table 1. As a result, part of the mixing water is rapidly absorbed by the brick particles, effectively reducing the amount of free water available for gypsum hydration and accelerating the setting process. This interpretation is further supported by microstructural observations (see Section 3.4), where the presence of voids and porous

WB particles was noted, suggesting that the fresh mortar matrix may experience localized water depletion around the brick fragments.

Moreover, the faster setting time may be linked to the reduction in total binder content as gypsum is progressively replaced. While the WB behaves as an inert filler and does not contribute to the hydration reaction, it increases the surface area within the mixture, further promoting localized stiffening [33,34]. These effects collectively shorten the interval between the initial and final setting, which drops from 15 min in M1 to less than 6 min in the WB-containing mortars.

It is important to highlight that, despite this acceleration, all the mortars met the standard requirements for setting time according to the standard NBR 13207:1994 [35], which states that gypsum plasters for coatings must have an initial setting time greater than 10 min and a final setting time greater than 45 min. However, the reduced working time in mixes with higher WB content, which approaches the minimum threshold of the standard [35], may affect their applicability in construction practices, particularly where extended setting time is required [36,37].

3.2. Water Absorption by Immersion

Figure 5 shows the water absorption by immersion of the gypsum mortars at 28 days of curing.

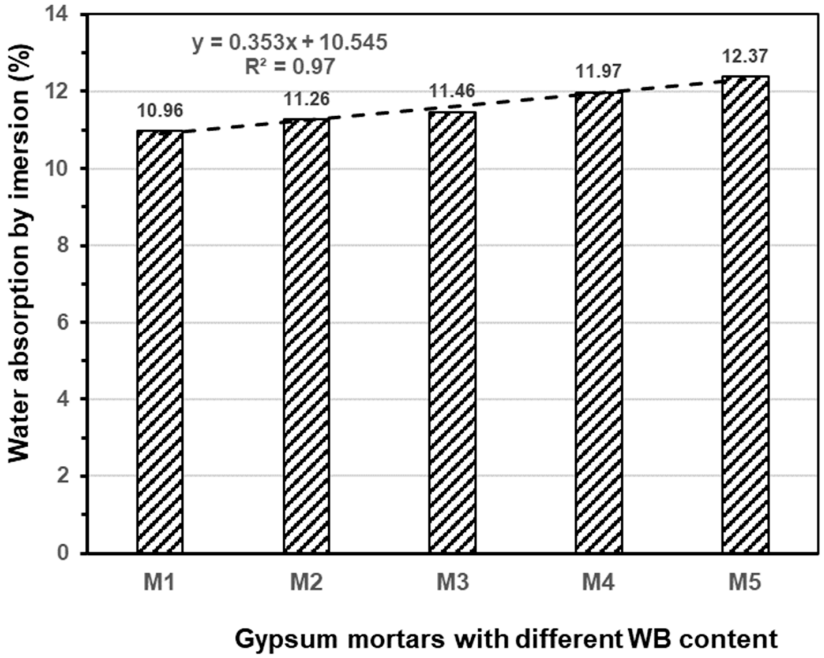

Figure 5. Water absorption by immersion for all the mortar compositions with and without the WB.

The reference mortar M1, which contains only gypsum as a binder, exhibits an absorption rate of approximately 11%. This value is consistent with the known porous nature of gypsum-based materials, which tend to retain water due to their microcapillary structure and relatively low density [38].

With the progressive replacement of gypsum by WB, a gradual increase in water absorption is observed. This behavior is attributed to the intrinsic characteristics of the WB, which, according to the material data in Table 1, has a water absorption capacity of nearly 29%. The high porosity and irregular surface texture of the crushed brick particles enhance the ability of the mortar to absorb and retain water within the matrix. These findings are in line with previous studies on mortars incorporating ceramic waste. For example, Ma et al. [33] reported a similar trend in cement-based composites, where increasing the content

of finely ground waste brick powder led to higher water absorption due to the high internal porosity and irregular surface of the particles. In that study, mortars with 20–30% brick powder showed absorption increases of up to 40% compared to the reference mix. Similarly, Naceri and Hamina [39] observed that waste brick aggregates increased porosity and capillary absorption in blended mortars, although the mechanical performance remained acceptable under dry conditions.

Furthermore, Scheinherrová et al. [36] emphasized that the porous and heterogeneous nature of ceramic residues contributes significantly to water retention when incorporated into gypsum- and lime-based matrices. Their study also indicated that while ceramic particles may not participate in hydration reactions, they alter the pore structure in a way that affects both water transport and vapor diffusion within the hardened material.

Regression analysis of the water absorption data yielded the following linear Equation (2):

$$\text{Absorption} = 0.353 \times \text{WB} + 10.545 \quad (2)$$

where absorption is a percentage, WB is expressed as fraction and $R^2 = 0.977$. The positive slope indicates that increasing the proportion of waste brick leads to a consistent rise in absorption. For every 1% increase in waste brick content, the water absorption increases in the gypsum mortars by approximately 0.353%. This result confirms a strong linear correlation between the waste brick content and the water absorption of gypsum mortar at 28 days, mainly due to the high porosity and absorptivity of the waste material compared to natural sand.

Despite the increase in absorption, the values remain within acceptable limits for non-structural applications, especially in interior environments.

3.3. Mechanical Properties

3.3.1. Flexural Strength

The flexural strength of the mortars as a function of WB content and curing time is shown in Figure 6.

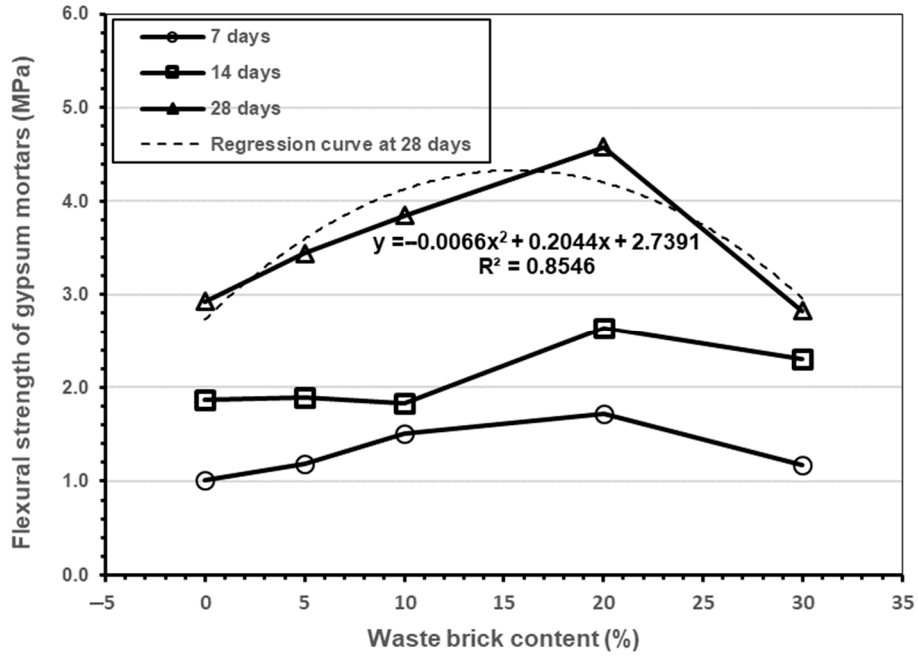

Figure 6. Flexural strength versus WB content at different curing times.

A clear improvement in flexural strength was observed with increasing WB content up to 20%, regardless of curing age. At 7 days, mortar M4 (i.e., 20% of WB) showed an increase of approximately 70% compared to the reference mortar M1; at 14 and 28 days, the gains were around 41% and 56%, respectively. Beyond this replacement level, the performance dropped: M5 (i.e., 30% of WB) showed reduced strength, falling below the 20% optimum but remaining comparable to or slightly above the reference in some cases.

This trend can be attributed to the microstructural effects induced by the addition of WB. As will be discussed in Section 3.3, the irregular and angular shape of the brick particles may enhance mechanical interlocking within the gypsum matrix, especially when present in moderate amounts. The increased roughness and heterogeneity at the aggregate–matrix interface likely contribute to more efficient stress transfer, thus improving flexural strength.

However, when the WB content exceeds 20%, the decrease in gypsum content reduces the amount of reactive binder, limiting matrix cohesion. Moreover, the high water absorption of WB may lead to localized water deficiencies during setting, hindering the complete formation of gypsum hydration products. This is consistent with the observations in the setting time tests (in Section 3.1), where faster setting was observed for higher WB contents.

The regression analysis of the data for the 28-day flexural strength shows that the flexural strength increases with waste brick content up to about 15–20%, then decreases beyond that. Therefore, the optimal waste brick content (for the highest 28-day strength) is approximately 17%. The R^2 obtained indicates a strong correlation and shows that the regression is a good representation of the actual behavior. The initial increase in strength may be due to improved microstructure as previously mentioned. Beyond about 15–20%, the excessive waste may reduce bonding or increase porosity (waste bricks have high water absorption (28.90%) compared to natural sand), leading to a drop in strength.

Overall, the results indicate that 20% WB replacement offers the best balance between mechanical reinforcement and binder dilution, in agreement with previous research on ceramic waste addition to gypsum composites [19].

3.3.2. Compressive Strength

The compressive strength results, reported in Figure 7, show a similar trend to that of flexural strength.

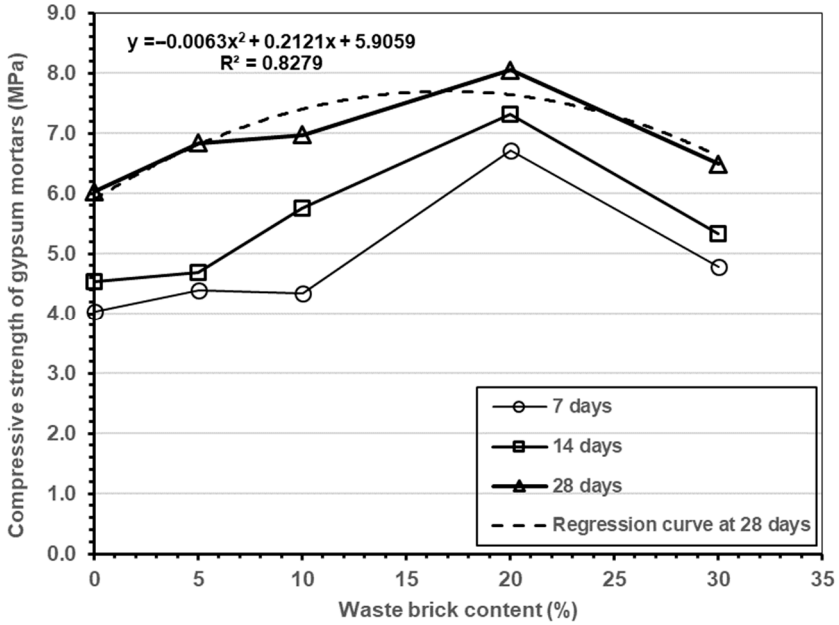

Figure 7. Compressive strength versus WB content at different curing times.

Up to 10% WB, the performance remains close to that of the reference mortar. At 20% WB, a significant improvement is observed: compressive strength increased by approximately 60% at 7 and 14 days and by 33% at 28 days, compared to M1.

This improvement is likely due to a combination of factors. First, the fine brick powder may act as a micro-filler, partially densifying the matrix and reducing voids. Second, the reduced water-to-binder ratio (as reported in Table 2) may have led to lower initial porosity, as less free water was available for evaporation during curing. Finally, the irregular shape of WB particles may again play a role in enhancing particle packing and stress distribution.

Nevertheless, at 30% WB (i.e., M5), the compressive strength drops, though it remains above the reference mix. This suggests that beyond 20%, the dilution of the binder dominates the mechanical response, and the filler effect of WB is no longer sufficient to compensate for the lack of cohesive phases. These results support the use of up to 20% WB as a sustainable and technically effective partial replacement of gypsum in mortars designed for non-structural applications.

The 28-day compressive strength of gypsum mortar exhibits a parabolic relationship with brick waste content, peaking at approximately 17% replacement. The quadratic regression model (R^2 = 0.8279) suggests a significant non-linear trend, where strength first increases and then decreases with higher substitution rates. The initial improvement can be attributed to the fineness of the waste brick powder, helping to fill tiny gaps between particles, which makes the mortar structure more solid and compact. Additionally, the irregular shape of the waste particles likely enhances mechanical interlocking and particle packing, improving stress distribution within the hardened matrix. These effects together promote a denser, more cohesive microstructure.

3.3.3. Adhesion Strength

Figure 8 presents the results of the adhesion strength test. The sample was tested at 28 days, and a progressive decline in the adhesion with increasing WB content was obtained.

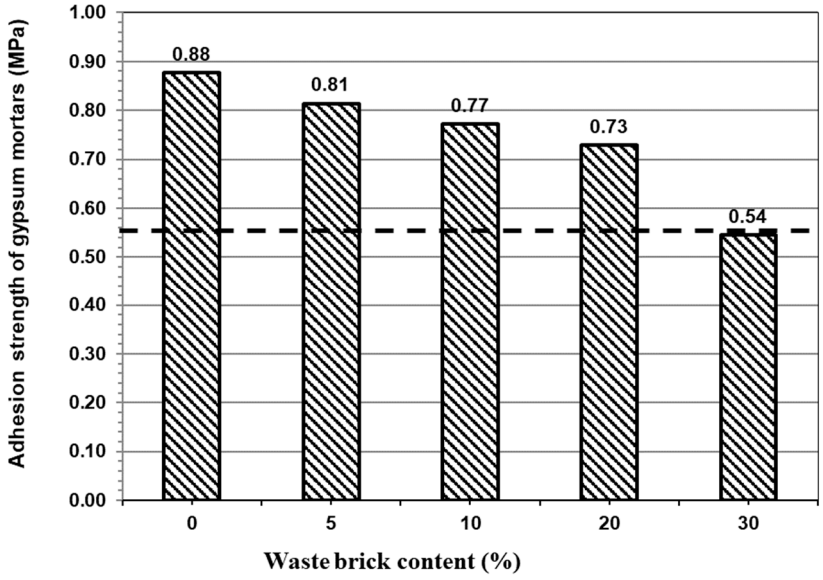

Figure 8. Adhesion strength of gypsum mortars versus WB content at the age of 28 days.

Mortar M1 showed the highest adhesion value (i.e., 0.88 MPa), followed by a gradual decline in mortars M2 to M5. At 20% WB (i.e., M4), adhesion was reduced to 0.73 MPa. With 30% WB (i.e., M5), the adhesion dropped significantly below the threshold of 0.57 MPa, typically required for gypsum mortars used in plasters and coatings.

This reduction can be explained by several concurrent effects. As the gypsum content decreases, the volume of binder available to create a cohesive interface with the substrate is reduced. Simultaneously, the increased porosity and water retention introduced by WB, evident in Sections 3.1 and 3.4, may weaken the bond between the mortar and the limestone substrate used for testing.

It is also possible that the faster setting observed in WB-rich mortars (in Section 3.1) negatively affects adhesion. Rapid loss of workability can limit the quality of contact with the substrate during application, especially when performed manually. For these reasons, maintaining WB content at or below 20% appears to be a reasonable compromise, allowing for improved strength and environmental performance without critically compromising adhesion.

3.4. Microstructural Characterization

A combined optical and scanning electron microscopy (SEM) investigation was conducted to assess the morphology, surface texture, and homogeneity of the mortar samples. Optical microscopy at 20× magnification revealed generally homogeneous and compact surfaces across all formulations, as can be observed in Figure 9.

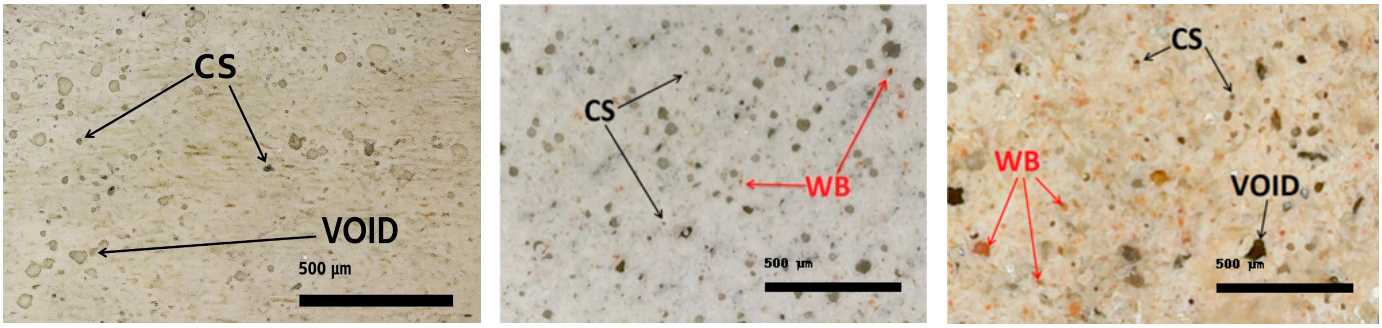

M1 M4 M5

Figure 9. Mortars' microstructure morphology obtained by optical microscopy with a magnification of 20× (CS = concrete sand; WB = waste brick).

Rounded sand particles and irregular fragments of waste brick (WB) were visually identifiable, with an increased coarseness observed in mortars containing higher WB content (i.e., M5). The presence of voids was also noted, likely resulting from entrapped air or excess water during casting. Surface coloration varied noticeably with WB content: the control mortar (M1) appeared light in tone, while mortars M4 and M5 showed a reddish hue due to the ceramic particles.

Optical microscopy revealed that all mortar samples containing waste brick as a partial replacement for gypsum exhibited generally homogeneous and compact surfaces. The microstructure appeared continuous, with minimal surface discontinuities or visible defects. In formulations with higher proportions of waste brick, slight increases in surface roughness and isolated pores were observed, possibly due to the irregular shape and granulometry of the recycled material. However, no significant cracks or delamination zones were detected, indicating good visual cohesion at the microscale. These observations suggest that the incorporation of waste brick did not adversely affect the surface uniformity of the mortar under optical magnification.

SEM analysis provided higher-resolution insights into the mortar microstructure. In the control sample (i.e., M1), shown in Figure 10, smooth gypsum crystals and microcline grains from sand were clearly distinguished.

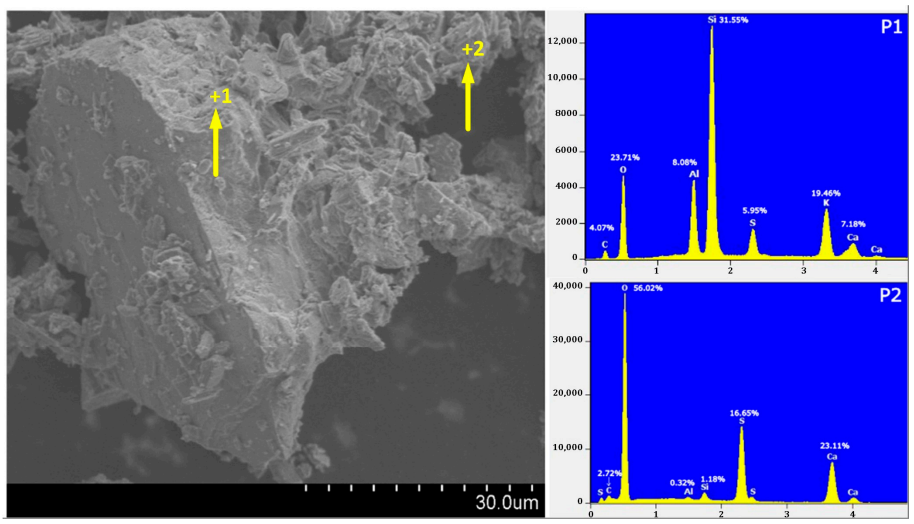

Figure 10. SEM images and EDS analysis of reference mortar (M1).

In contrast, the M5 sample exhibited a more heterogeneous morphology, with angular and irregular quartz particles likely originating from either sand or WB, as reported in Figure 11.

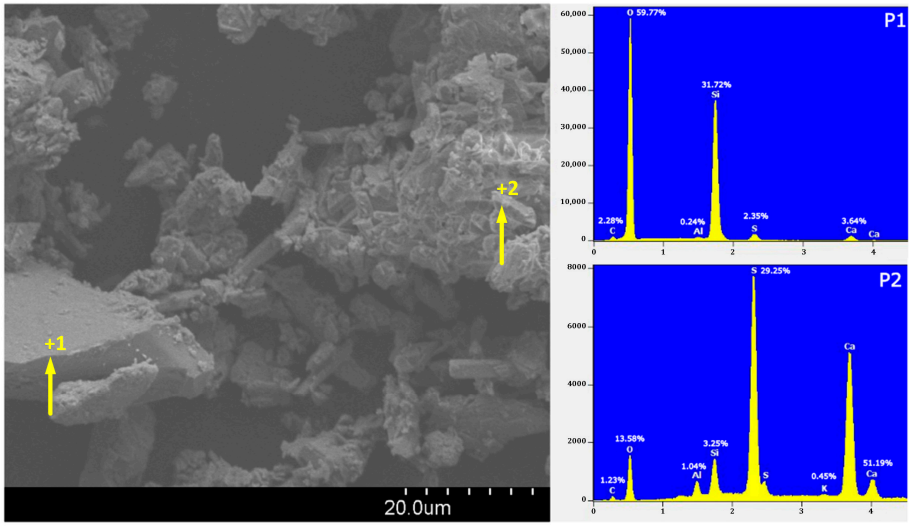

Figure 11. SEM images and EDS analysis of mortar with the higher amount of WB (M5).

EDS analysis confirmed the elemental composition of selected areas, identifying gypsum (Ca and S) and quartz (Si and O) as the predominant phases. No new crystalline phases were detected in SEM or XRD, indicating that WB acts as an inert filler within the matrix, without undergoing significant chemical interaction with gypsum. These observations are consistent with previous studies [23,33,40].

3.5. X-Ray Diffraction Analysis

X-ray diffraction (XRD) was conducted on the hardened gypsum mortars after 28 days of curing to assess their mineralogical composition, as shown in Figure 12.

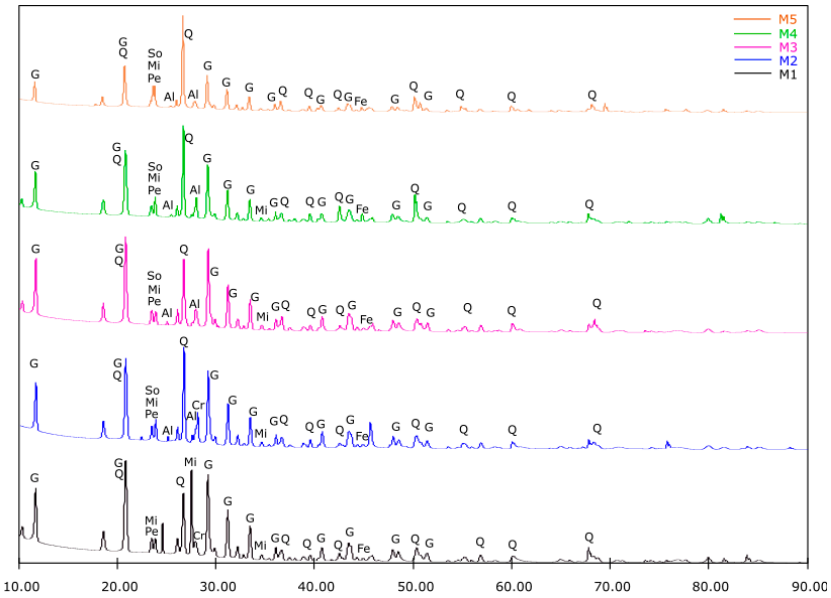

Figure 12. XRD patterns of mortar compositions with and without WB. Al: albite (COD: 2107372), Cr: cristobalite (COD: 1010921), Fe: iron (COD: 9013463), G: gypsum (COD: 1010981), Mi: microcline (COD: 9000943), Pe: petalite (COD: 9008304), Q: quartz (COD: 1011097), So: sodalite (COD: 1011139).

All samples displayed bassanite (G), the primary phase derived from the commercial gypsum binder, especially prominent around 2θ ≈ 14.7°, 25.5°, and 29.7°. As the proportion of waste brick (WB) increases, the intensity of these bassanite peaks progressively decreases, in line with the reduced gypsum content in the mixtures. Quartz (Q) is consistently present in all formulations, showing sharp peaks at 2θ ≈ 20.8°, 26.6°, 36.5°, 39.5°, 50.2°, and 60.0°, originating from both sand and WB. Microcline (Mi) appears primarily between 2θ ≈ 27.3° and 30.0°, and petalite (Pe) is detected in a broader range near 2θ ≈ 22–25°. Traces of iron (Fe) are also present, with peaks observable near 2θ ≈ 44.7°, consistent with the natural sand composition.

In mortars containing waste brick (M2 to M5), additional crystalline phases such as sodalite (So) were detected, around 2θ ≈ 24.5° and 35.0°, reflecting the contribution of ceramic waste. An interesting trend was observed in the distribution of cristobalite (Cr) and albite (Al): cristobalite was clearly present in M1 and marginally in M2, with characteristic peaks near 2θ ≈ 22.0° and 36.1°, but progressively disappeared in mortars with higher WB content. This shift is attributed to the increasing presence of albite, whose diffraction peaks overlap with those of cristobalite, making it the dominant feldspar phase in mixes with 10% WB or more.

The progressive appearance of albite and sodalite, without the formation of new or unexpected phases, suggests that WB behaves as an inert addition at the mineralogical level. This finding is consistent with the SEM-EDS results discussed in Section 3.4, which revealed no evidence of reaction products or changes in crystal morphology due to the presence of WB. The XRD patterns thus confirm that the incorporation of waste brick does not interfere with the hydration of gypsum, as bassanite remains the predominant phase in all formulations.

From a chemical compatibility standpoint, the coexistence of gypsum-derived and ceramic-derived minerals without new phase formation is favorable for the stability of the material. The inert nature of the WB also contributes to dimensional stability and reduces the risk of deleterious reactions over time. However, this same lack of reactivity implies that the WB does not participate in any pozzolanic or cementitious reactions within the matrix. Although literature has shown that finely ground fired clay bricks can exhibit

pozzolanic activity in the presence of calcium-rich binders such as lime or cement, in the case of pure gypsum matrices, the pH and mineral environment are generally not sufficient to activate such behavior [19,36,41].

3.6. Environmental Impact

The environmental performance of the gypsum mortars was assessed by evaluating the Global Warming Potential (GWP, expressed in kg CO_2 eq per cubic meter of mortar) and energy demand associated (expressed in MJ/m^3) with each formulation, based on a cradle-to-gate approach.

This assessment was performed using the actual compositions of each mortar (M1 to M5, reported in Table 2) and a functional unit of 1 m^3 of finished product.

Emission and energy factors for the raw materials were sourced from literature and life cycle databases (i.e., Ecoinvent and European Life Cycle Database, ELCD). For natural gypsum, a GWP of 210 kg CO_2 eq/t and an energy demand of 3500 MJ/t were used, based on the ELCD and corroborated by Fořt and Černý [18]. The contribution of recycled waste brick was estimated using values of 24 kg CO_2 eq/t and 200 MJ/t, reflecting its low environmental impact as a construction and demolition (C&D) by-product [33,36,39]. For construction sand, average values of 10 kg CO_2 eq/t and 200 MJ/t were adopted based on ELCD and supported by Rosado et al. [42]. The superplasticizer, based on a polyacrylate admixture, was associated with a GWP of 1100 kg CO_2 eq/t and an energy demand of 20,000 MJ/t, as reported by Ecoinvent. Water was considered with minimal impact, using 0.4 kg CO_2 eq/t and 5 MJ/t as average values for tap water (as reported on ELCD).

It is worth noting that some of the energy and emission factors used for WB were obtained from the literature, which already accounts for common life cycle stages such as crushing, sieving, and drying [36,43]. However, process-specific variations and on-site conditions are not captured, which represents a limitation of this study. A sensitivity analysis was not carried out, as the purpose of this assessment was to provide a comparative estimate based on standard cradle-to-gate data. Furthermore, the literature data suggest that additional energy requirements for grinding and drying are relatively low (i.e., 5–10 MJ/kg of material), and would not significantly alter the relative environmental trends observed. Nonetheless, this remains a source of uncertainty and should be considered when interpreting the results.

The calculated values of GWP and energy demand for each mortar formulation are reported in Table 3.

Table 3. Environmental impact of gypsum mortars (for 1 m^3 of finishing material).

Sample	GWP (kg CO_2 eq/m^3)	Energy Demand (MJ/m^3)
M1	221.80	3795.04
M2	214.28	3662.45
M3	206.77	3529.83
M4	191.72	3264.39
M5	176.65	2998.76

The reference mortar M1, made entirely with natural gypsum as a binder, exhibited the highest GWP value (i.e., 221.80 kg CO_2 eq/m^3). A progressive reduction was observed with increasing WB content, reaching 176.65 kg CO_2 eq/m^3 for M5 (i.e., 30% WB), which represents a 20% decrease compared to M1. This improvement is directly linked to the replacement of gypsum, a material requiring high-temperature calcination, with a recycled ceramic filler that demands minimal processing.

Energy demand followed a similar trend, decreasing from 3795.04 MJ/m^3 in M1 to 2998.76 MJ/m^3 in M5, with a total reduction of approximately 21%. This reflects the lower embodied energy of the WB powder and the lower binder content in the formulations with higher substitution levels.

These results confirm that the partial replacement of gypsum with WB can significantly reduce both the GWP and energy consumption, supporting the development of more sustainable mortars.

4. Conclusions

This study investigated the technical and environmental performance of gypsum mortars in which natural gypsum was partially replaced by waste brick (WB) powder at different levels (0–30% by weight). The objective was to evaluate the feasibility of using WB as a sustainable alternative binder in non-structural construction applications.

The investigation led to the following results:

- The setting time consistently decreased with increasing WB content, due to the high water absorption capacity of the brick particles, which reduces the availability of free water for gypsum hydration.
- Water absorption also increased with WB content, although values remained within acceptable limits for interior applications.
- Mechanical testing showed that the flexural and compressive strengths improved with WB content up to an optimal level of 20%, likely due to enhanced particle packing and mechanical interlocking. Beyond this level, the dilution of the binder reduced performance, particularly in terms of adhesion strength, which dropped significantly at 30% WB. Nevertheless, mortars containing up to 20% WB maintained acceptable adhesion values and showed superior strength compared to the reference mix.
- Microstructural characterization by optical microscopy and SEM revealed that the addition of WB increases heterogeneity and introduces irregular, porous particles that do not chemically interact with gypsum, as confirmed by EDS and XRD analysis.
- Environmental assessment based on cradle-to-gate life cycle data demonstrated that the partial replacement of gypsum with WB led to a reduction of up to 20% in Global Warming Potential and 21% in energy consumption per cubic meter of mortar. These results confirm the environmental benefits of incorporating recycled ceramic waste into gypsum-based products, particularly in the mix with 20% WB, which offered the best compromise between technical and environmental performance.

In conclusion, the use of WB as a partial substitute for gypsum is a viable and sustainable solution for the production of eco-efficient mortars. Future studies may explore the long-term durability of these materials under environmental exposure, as well as their performance in historical restoration applications or hybrid formulations with other recycled components.

Author Contributions: Conceptualization, S.B., R.-M.I., A.B. and M.A.O.; methodology, S.B., A.B. and M.A.O.; validation, A.S., A.B. and R.-M.I.; formal analysis, A.S., S.B., M.A.O. and K.N.; investigation, S.B. and K.N.; resources, S.B.; data curation, A.S. and S.B.; writing—original draft preparation, S.B. and M.A.O.; writing—review and editing, A.S., A.B. and K.N.; visualization, A.S., S.B., A.B. and, M.A.O.; supervision, A.S. and A.B. All authors have read and agreed to the published version of the manuscript.

Funding: This research received no external funding.

Institutional Review Board Statement: Not applicable.

Informed Consent Statement: Not applicable.

Data Availability Statement: The data presented in this study are available in the article. Further inquiries can be directed to the corresponding author.

Acknowledgments: The authors would like to thank the Francophone University Agency (Agence Universitaire de la Francophonie) in Romania for supporting this research through its scientific cooperation and mobility program.

Conflicts of Interest: The authors declare no conflicts of interest.

Abbreviations

The following abbreviations are used in this manuscript:

WB	Waste Brick
SEM	Scanning Electron Microscope
EDS	Energy Dispersive Spectroscopy
XRD	X-Ray Diffraction
XRF	X-Ray Fluorescence
CDW	Construction and Demolition Waste
RCAs	Recycled Concrete Aggregates
RCBP	Recycled Clay Brick Powder
G	Gypsum
CS	Construction Sand
SP	Superplasticizer
GWP	Global Warming Potential

References

1. Soto-Paz, J.; Arroyo, O.; Torres-Guevara, L.E.; Parra-Orobio, B.A.; Casallas-Ojeda, M. The Circular Economy in the Construction and Demolition Waste Management: A Comparative Analysis in Emerging and Developed Countries. *J. Build. Eng.* **2023**, *78*, 107724. [CrossRef]
2. Aslam, M.S.; Huang, B.; Cui, L. Review of Construction and Demolition Waste Management in China and USA. *J. Environ. Manag.* **2020**, *264*, 110445. [CrossRef]
3. Zhang, C.; Hu, M.; Di Maio, F.; Sprecher, B.; Yang, X.; Tukker, A. An Overview of the Waste Hierarchy Framework for Analyzing the Circularity in Construction and Demolition Waste Management in Europe. *Sci. Total Environ.* **2022**, *803*, 149892. [CrossRef]
4. Ginga, C.P.; Ongpeng, J.M.C.; Daly, M.K.M. Circular Economy on Construction and Demolition Waste: A Literature Review on Material Recovery and Production. *Materials* **2020**, *13*, 2970. [CrossRef] [PubMed]
5. Hu, J.; Ahmed, W.; Jiao, D. A Critical Review of the Technical Characteristics of Recycled Brick Powder and Its Influence on Concrete Properties. *Buildings* **2024**, *14*, 3691. [CrossRef]
6. Sinkhonde, D. Energy Assessments of Concrete Incorporating Waste Tire Rubber and Waste Brick Powder: A Comparative Analysis of Various Concrete Grades. *Clean. Energy Syst.* **2024**, *8*, 100115. [CrossRef]
7. Silva, R.V.; de Brito, J.; Dhir, R.K. Use of Recycled Aggregates Arising from Construction and Demolition Waste in New Construction Applications. *J. Clean. Prod.* **2019**, *236*, 117629. [CrossRef]
8. Zhou, Y.; Wang, R. Application of the Supplementary Cementitious Material and Aggregates Made from Waste Clay Bricks in the Preparation of Plastering Mortar. *Constr. Build. Mater.* **2024**, *450*, 138705. [CrossRef]
9. Raini, I.; Raini, I.; El Bougrini, A.; Cherifi, H.; El Qandil, M. Valorization of Concrete and Brick Waste as Sustainable Alternatives in Lime Mortar: Physical, Mechanical, and Durability Performance. *J. Ecol. Eng.* **2025**, *26*, 40–53. [CrossRef]
10. Liu, Y.; Mehdizadeh, H.; Ling, T.-C. Improved Concrete ITZ and Performance via Pre-Soaking of Inert Recycled Red Brick Aggregates in Carbonation Solution. *J. Build. Eng.* **2024**, *86*, 108961. [CrossRef]
11. Li, J.; Feng, H.; Liu, Y.; Zhang, J.; Ma, Y.; Ma, T. Determining the Optimal Gradation of Mixed Recycled Aggregate Containing Coal Gangue Brick Aggregate. *Case Stud. Constr. Mater.* **2024**, *20*, e02968. [CrossRef]
12. Guo, K.; Dong, H.; Zhang, J.; Zhang, L.; Li, Z. Experimental Study of Alkali-Activated Cementitious Materials Using Thermally Activated Red Mud: Effect of the Si/Al Ratio on Fresh and Mechanical Properties. *Buildings* **2025**, *15*, 565. [CrossRef]
13. Li, Z.; Dong, H.; Zhao, X.; Wang, K.; Gao, X. Utilisation of Bayer Red Mud for High-Performance Geopolymer: Competitive Roles of Different Activators. *Case Stud. Constr. Mater.* **2025**, *23*, e05047. [CrossRef]
14. Chen, X.-F.; Zhang, X.-C.; Peng, Y. Recycled Clay Brick Powder as a Dual-Function Additive: Mitigating the Alkali–Silica Reaction (ASR) and Enhancing Strength in Eco-Friendly Mortar with Hybrid Waste Glass and Clay Brick Aggregates. *Materials* **2025**, *18*, 2838. [CrossRef] [PubMed]
15. Kilumile, M.; Barra, M.; Mohamed, F.; Aponte, D. Use of Recycled Aggregates in Lime Mortars for Conservation of Historical Buildings. *Constr. Mater.* **2025**, *5*, 28. [CrossRef]

16. Sallı Bideci, Ö.; Bideci, A.; Ashour, A. Utilization of Recycled Brick Powder as Supplementary Cementitious Materials—A Comprehensive Review. *Materials* **2024**, *17*, 637. [CrossRef]
17. Zou, Z.; Provoost, S.; Gruyaert, E. Utilization of Waste Brick Powder as a Partial Replacement of Portland Cement in Mortars. *Sustainability* **2024**, *16*, 624. [CrossRef]
18. Fořt, J.; Černý, R. Carbon Footprint Analysis of Calcined Gypsum Production in the Czech Republic. *J. Clean. Prod.* **2018**, *177*, 795–802. [CrossRef]
19. del Río-Merino, M.; Vidales-Barriguete, A.; Piña-Ramírez, C.; Vitiello, V.; Santa Cruz-Astorqui, J.; Castelluccio, R. A Review of the Research about Gypsum Mortars with Waste Aggregates. *J. Build. Eng.* **2022**, *45*, 103338. [CrossRef]
20. Kethiri, M.A.; Belghar, N.; Chikhi, M.; Boutera, Y.; Beldjani, C.; Tedeschi, C. Experimental Study on the Effect of Date Palm Powder on the Thermal and Physico-Mechanical Properties of Gypsum Mortars. *Sustainability* **2024**, *16*, 3015. [CrossRef]
21. Fernandez, F.; Insinga, M.G.; Basile, R.; Zagarella, F.; Montagno, R.; Germanà, M.L. Comparative Evaluation of Gypsum-Based Plasters with Pistachio Shells for Eco-Sustainable Building. *Sustainability* **2024**, *16*, 3695. [CrossRef]
22. Beldjilali, S.; Bougara, A.; Aguiar, J.; Bouhamou, N.-E.; Dabbebi, R. Properties of a New Material Based on a Gypsum Matrix Incorporating Waste Brick. *Constr. Build. Mater.* **2020**, *259*, 120416. [CrossRef]
23. Naciri, K.; Aalil, I.; Chaaba, A. Eco-Friendly Gypsum-Lime Mortar with the Incorporation of Recycled Waste Brick. *Constr. Build. Mater.* **2022**, *325*, 126770. [CrossRef]
24. *BS EN 13279-1:2008*; Gypsum Binders and Gypsum Plasters Definitions and Requirements. European Standards: Brussels, Belgium, 2008.
25. *EN 1015-3*; Methods of Test for Mortar for Masonry—Part 3: Determination of Consistence of Fresh Mortar (by Flow Table). CEN: Brussels, Belgium, 2004.
26. *EN 998-1*; Specification for Mortar for Masonry—Part 1: Rendering and Plastering Mortar. CEN: Brussels, Belgium, 2010.
27. *EN 1015-11*; Methods of Test for Mortar for Masonry—Part 11: Determination of Flexural and Compressive Strength of Hardened Mortar. CEN: Brussels, Belgium, 1999.
28. *EN 1015-12:2000*; Methods of Test for Mortar for Masonry—Part 12: Determination of Adhesive Strength of Hardened Rendering and Plastering Mortars on Substrates. CEN: Brussels, Belgium, 2000.
29. *ASTM C191-04*; Standard Test Method for Time of Setting of Hydraulic Cement by Vicat Needle. ASTM International: West Conshohocken, PA, USA, 2017.
30. *BS EN 1015-182002 3*; Methods of Test for Mortar for Masonry-Part 18: Determination of Water Absorption Coefficient Due to Capillary Action of Hardened Mortar. British Standard: London, UK, 2002.
31. Racataianu, P.; Koch, R. Dimension Stones of the Old City Wall of Cluj-Napoca, Romania—An Overview on History, Mapping, Weathering, and Damages. *Stud. UBB Geol.* **2009**, *54*, 17–22. [CrossRef]
32. Onuțu, C.; Ungureanu, D.; Isopescu, D.N.; Vornicu, N.; Spiridon, I.A. Sourcing Limestone Masonry for the Restoration of Heritage Buildings: Frumoasa Monastery Case Study. *Materials* **2022**, *15*, 7178. [CrossRef]
33. Ma, Z.; Tang, Q.; Wu, H.; Xu, J.; Liang, C. Mechanical Properties and Water Absorption of Cement Composites with Various Fineness and Contents of Waste Brick Powder from C&D Waste. *Cem. Concr. Compos.* **2020**, *114*, 103758. [CrossRef]
34. Geraldo, R.H.; Pinheiro, S.M.M.; Silva, J.S.; Andrade, H.M.C.; Dweck, J.; Gonçalves, J.P.; Camarini, G. Gypsum Plaster Waste Recycling: A Potential Environmental and Industrial Solution. *J. Clean. Prod.* **2017**, *164*, 288–300. [CrossRef]
35. *NBR 13207*; Gypsum for Buildings—Specification. ABNT: Rio de Janeiro, Brazil, 1994. (In Portuguese)
36. Scheinherrová, L.; Doleželová, M.; Vimmrová, A.; Vejmelková, E.; Jerman, M.; Pommer, V.; Černý, R. Fired Clay Brick Waste as Low Cost and Eco-Friendly Pozzolana Active Filler in Gypsum-Based Binders. *J. Clean. Prod.* **2022**, *368*, 133142. [CrossRef]
37. Erbs, A.; Nagalli, A.; Querne de Carvalho, K.; Mymrin, V.; Passig, F.H.; Mazer, W. Properties of Recycled Gypsum from Gypsum Plasterboards and Commercial Gypsum throughout Recycling Cycles. *J. Clean. Prod.* **2018**, *183*, 1314–1322. [CrossRef]
38. del Río Merino, M.; Santa Cruz Astorqui, J.; Villoria Sáez, P.; Santos Jiménez, R.; González Cortina, M. Eco Plaster Mortars with Addition of Waste for High Hardness Coatings. *Constr. Build. Mater.* **2018**, *158*, 649–656. [CrossRef]
39. Naceri, A.; Hamina, M.C. Use of Waste Brick as a Partial Replacement of Cement in Mortar. *Waste Manag.* **2009**, *29*, 2378–2384. [CrossRef] [PubMed]
40. Khitab, A.; Riaz, M.S.; Jalil, A.; Khan, R.B.N.; Anwar, W.; Khan, R.A.; Arshad, M.T.; Kirgiz, M.S.; Tariq, Z.; Tayyab, S. Manufacturing of Clayey Bricks by Synergistic Use of Waste Brick and Ceramic Powders as Partial Replacement of Clay. *Sustainability* **2021**, *13*, 10214. [CrossRef]
41. Krejsová, J.; Schneiderová Heralová, R.; Doleželová, M.; Vimmrová, A. Environmentally Friendly Lightweight Gypsum-Based Materials with Waste Stone Dust. *Proc. Inst. Mech. Eng. Part L J. Mater. Des. Appl.* **2019**, *233*, 258–267. [CrossRef]

42. Rosado, L.P.; Vitale, P.; Penteado, C.S.G.; Arena, U. Life Cycle Assessment of Natural and Mixed Recycled Aggregate Production in Brazil. *J. Clean. Prod.* **2017**, *151*, 634–642. [CrossRef]
43. Simion, I.M.; Fortuna, M.E.; Bonoli, A.; Gavrilescu, M. Comparing Environmental Impacts of Natural Inert and Recycled Construction and Demolition Waste Processing Using LCA. *J. Environ. Eng. Landsc. Manag.* **2013**, *21*, 273–287. [CrossRef]